Human Adenovirus-Induced Medulloepitheliomatous Neoplasms in Sprague-Dawley Rats

Noritsugu Mukai, MD and Shoji Kobayashi, MD

A direct causal relationship between a human virus and malignant transformations in target cells (sensory neuronal precursors) was suggested by the development of a medulloepitheliomatous neoplasm in the central nervous system. Twenty-six newborn Sprague-Dawley rats were given a single intracerebral inoculation of 0.05 ml of adenovirus fluid, $10^{3.5}$ to $10^{4.5}$ $TCID_{50}$ HeLa cells/0.1 ml, in the left frontal lobe. Within 37 to 151 days after the virus inoculation, 23 (88.7%) rats autochthonously developed an adenovirus-typical neoplasm in the central nervous system. Nine animals developed a multicentric neoplasm closely related to the ventricular system. Nine others developed solid variously sized neoplasms along the ventricular lumen. Some neoplasms showed multiple foci connected with the stratum subependymale ventriculi olfactorii and the velum medullare of the fourth ventricle. Six spinal cord tumors, located chiefly in the dorsal sensory column, developed within 37 to 61 days after intracerebral inoculation. The remarkably uniform histopathologic appearance of all 23 cases was attributed to a medulloepitheliomatous neoplasm derived from the ependymal anlage. Electron microscopy clearly revealed a solitary cilium within the apical region of many tumor cells. It consisted of a typical ring of nine doublets with no axial pair (a 9+0 pattern), the typical structure of cilia of sensory neuronal origin. The appearance of exuberant neuron-like tumor cells with argyrophile cytoplasmic expansions, neurosyncytial mosaic alignment and myelin-like configurations also suggested a neuronal origin. A paucity of mesenchymal stroma in the neoplastic tissue was noted. No control animals developed tumors (Am J Pathol 73:671–690, 1973).

SINCE THE ORIGINAL PROTOTYPE of human adenovirus type 12 was isolated in primary human embryo kidney cultures from a child born in Boston,[1,2] this unique DNA virus has been one of the important groups of human viruses chosen for study of viral oncogenesis. This is because the virus is latent in a large percentage of children,[3–5] and also because it is similar to some known animal viruses, such as polyoma virus. The discovery by Trentin *et al*[6] of the oncogenic potential of human adenovirus type 12 in Syrian hamsters provided the first evidence

From the Wesley C. Bowers Laboratory of Pharmacology and Experimental Pathology, Department of Retina Research, Retina Foundation, Boston, Mass.

Supported by Research Grants EY-00227 from the National Eye Institute and CA-12180 from the National Cancer Institute, US Public Health Service, by grants from Fight for Sight, Inc, New York, Research to Prevent Blindness, Inc, and by the Massachusetts Lions Eye Research Fund, Inc.

Accepted for publication Aug 15, 1973.

Address reprint requests to Manuscript Editor, Retina Foundation, 20 Staniford St, Boston, MA 02114.

that a virus of human origin can induce a highly malignant neoplasm.

In a previous communication [7] we reviewed 26 articles dealing with adenovirus-typical neoplasms. None of them was successful in proving incontrovertibly that the target cell in adenovirus tumorigenesis originates from a definite neuron precursor cell group. Furthermore, no animal model of highly reproducible embryonal neuronal tumors utilizing common laboratory animals was provided. The purpose of this paper is to present the first successful animal model of a medulloepitheliomatous neoplasm in randomly bred Sprague-Dawley rats. This animal model may provide an excellent system in which to study not only chemotherapeutic effects but also the basic mechanisms that allow malignant transformation of differentiating cells in the central nervous system, as may occur in its human counterpart.

Materials and Methods

Preparation of Concentrated Virus Fluid

Human adenovirus type 12 (Huie Strain, Flow Laboratories, Rockville, Md) was cultured in a HeLa cell monolayer prepared as described previously.[7]

Inoculation of Virus Fluid

Twenty-six newborn, random-bred Sprague-Dawley rats (Charles River Breeding Laboratories, North Wilmington, Mass) were given a single intracerebral inoculation, in the left frontal lobe, of 0.05 ml of virus fluid, $10^{3.5}$ to $10^{4.5}$ $TCID_{50}$ HeLa cells/0.1 ml within 24 hours after birth. All inoculations were performed under an operating microscope with a fine hypodermic needle (No. 30, Metropolitan Supply, Cambridge, Mass) connected to a microsyringe (No. 710-N, Hamilton). Simple stereotactic maneuvering was performed after placing a fine vinyl tube of appropriate length on the needle. The tube functioned as a sheath which insured that the needle penetrated no further than a circumscribed subcortical area of the left frontal lobe. Twenty newborn control rats of the same strain were treated with 0.05 ml of supernatant fluid from non-virus-infected HeLa cells cultured in the same medium as that used in preparing the virus fluid. All animals were fed a balanced diet of pellets (General Biochemicals).

Histologic Examination

Paraffin sections were prepared from formalin-fixed (immersion) and formaldehyde-glutaraldehyde-fixed (perfusion) specimens. Epon-embedded sections were also prepared. Frozen sections were made with a cryostat. For cytologic identification, hematoxylin and eosin, phosphotungstic acid-hematoxylin, luxol fast blue, Foot's reticulin stain and Holmes' silver stain were used. Epon-embedded sections 2 μ thick were stained with 0.1% buffered toluidine blue. Cryosections were studied histochemically with NADH and NADPH tetrazolium oxidoreductases, ATPase, alkaline and acid phosphatases, luxol fast blue and acetylcholinesterase (Burstone).

Electron Microscopy

Seventeen animals were subjected to whole-body perfusion with Karnovsky's formaldehyde-glutaraldehyde fixative.[8] Perfused animal bodies were kept at 4 C for several hours. Slabs of dissected tumors, 5 mm thick, were fixed with the same solution at room temperature for 2 hours and were then diced into small blocks under a binocular microscope. The blocks were refixed with the same fixative for 2 to 5 hours and were then immersed overnight in 0.2 M phosphate buffer, pH 7.2, at 4 C. The blocks were postfixed with 2.0% osmium tetroxide and embedded in Epon-812. Ultrathin sections cut with an LKB-Ultrotome were stained with both uranyl acetate and lead citrate at 37 C for 45 minutes. Samples were studied with a Philips 200 and a Philips 300 electron microscope.

Results

Gross Findings

Direct intracerebral inoculation into the left frontal quiescent area of 26 newborn random-bred Sprague-Dawley rats resulted in 23 cases of brain and spinal cord tumors (88.7%) within 37 to 115 days after virus inoculation (Table 1). In 9 cases, variously sized solid tumors appeared haphazardly throughout both hemispheres and displayed close relationships to the ventricular system. In 9 other cases, the brain tumors consisted of multicentric medullary tumors along the line of the ventricular system (Text-figure 1). The most striking feature among these 9 cases was a multiple intraventricular tumor involvement that resulted in at least four entirely independent tumors (Text-figure 1, case 11). Another good example of a multicentric tumor, which is suggestive of simultaneous neoplastic growth, is illustrated in Figure 1.

At least five independent tumors were found between the olfactory bulb and the fourth ventricle (Figure 1, arrows). In the solid intraventricular tumors, part of the tumor mass was frequently contiguous to residual cells in the periventricular zone (Figure 2, long arrow). Futhermore, small incipient tumors with a close relationship to the stratum subependymale ventriculi olfactorii were found in the ventral horns and olfactory bulb (Figure 2, short arrows). In 4 of the 5 recorded cases of fourth ventricle tumors, these tumors were associated with other multiple solid tumors of the cerebral hemisphere (Text-figure 1, boldface numbers). Tumors occupying the entire lumen of the fourth ventricle appeared to have encroached upon part of the cerebellar folia. Occasionally, part of the tumor was contiguous to the tela choroidea and velum medullare posterius (Figures 3B and 5B).

Five cases of solid autochthonous gliomas of the spinal cord mainly localized in the dorsal column between Th-11 and S-1 developed within 37 to 61 days after injection (Table 1, cases 1 to 5 and 10). A

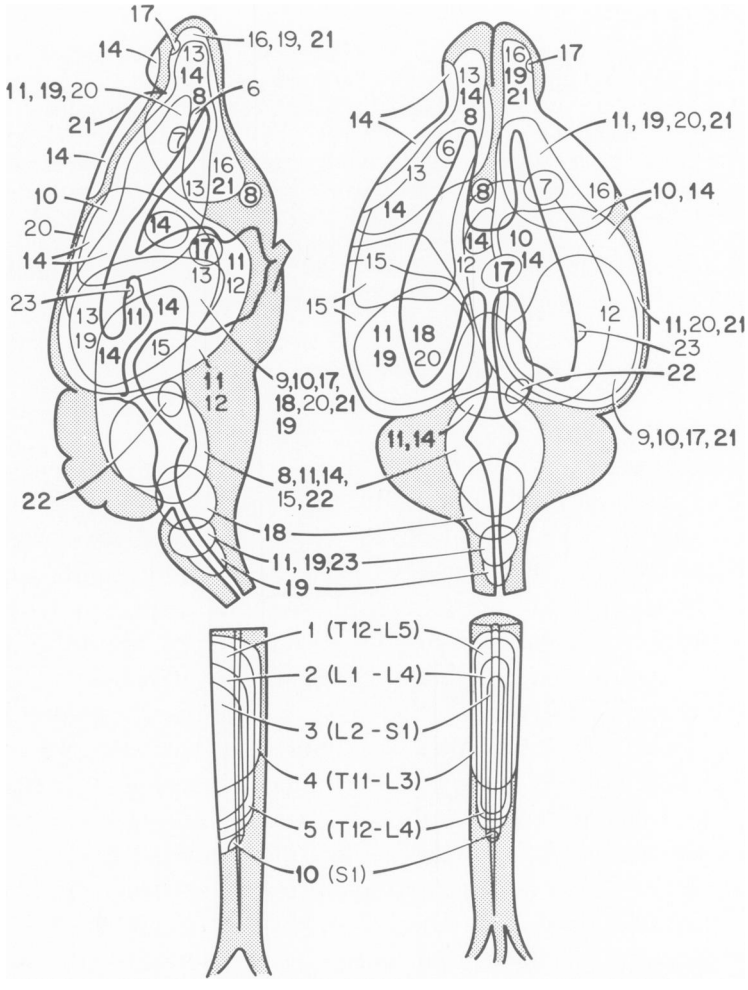

TEXT-FIG 1—Localization and distribution of tumors induced by a single virus inoculation. *Numbers in boldface* indicate cases with multiple tumors of multicentric origin.

nearly total *in situ* replacement of the lumbosacral region was found in three cases (Figure 4). Another small tumor (S-1) was found with a large hemispherical tumor (case 10). No control rats developed tumors.

Microscopic Findings

When viewed microscopically, the tumors were densely packed with syncytially aligned cells and appeared to have no connective tissue strands (Figures 5A and 6A). There was no marked tendency to subarachnoidal dissemination; a remarkably uniform cellular architecture, consisting of rosettes and perivascular cell wreaths formed by

slightly elongated unipolar cells, was characteristic of all cases (Figure 5). The neoplastic cells were occasionally found to be contiguous to a part of the tela choroidea and velum medullare (Figures 3B and 5B). Well-preserved choroid plexus epithelia were found in all tumors.

The vast majority of tumor cells retained high argentaffinity with no tendency to form reticulin or collagen stroma (Figure 6A). Bizarre neuronal cells associated with numerous fine argyrophilic protoplasmic expansions appeared to be distributed haphazardly throughout the tumor tissue (Figure 6B). Some giant cells formed an isolated focus merging into otherwise normally differentiated neurons in various sites in the cerebral cortices. A spine-like protuberance of these neuronal tumor cell processes was fairly common (Figure 6B). Mitotic figures were abundant, while there was little indigenous glial response to neoplastic cell invasion.

Histochemically, intense NADH-positive diformazan granules were detectable in tumor cell cytoplasm, whereas the NADPH response was feeble. Phospholipid content revealed by luxol fast blue was high in the tumor cell cytoplasm, as well as in the material between the closely packed syncytially interlacing tumor cells. Granules which responded positively to Burstone's substrate for cholinesterase were haphazardly distributed in and around the tumor cell cytoplasm, particularly in tumor cells that were closely aligned with newly vascularized areas.

Electron Microscopic Findings

Closely packed tumor cells forming a syncytial pattern or rosettes showed very few intercellular junction complexes and terminal bars. A slightly elongated unipolar cell body with an irregularly indented nucleus occupying a large portion of the cytoplasm was predominant throughout the specimens. Nucleoli were prominent, and occasionally, bizarre stippled aggregates of chromosomes were seen (Figure 8). The cytoplasmic organelles were poorly differentiated, with a number of mitochondria; free ribosomes were abundant (Figures 8–10). Within the apical region of the tumor cell cytoplasm, only one cilium, which displayed the typical concentric pattern of none pairs of peripheral doublets (tubules) without a central axial pair (9+0 pattern), was detected in all specimens (Figures 8 and 9, long arrows). No case was observed showing multiple cilia equipped with a complex of nine peripheral and two axial doublets. Well-developed intracytoplasmic microtubules and neurofilaments were commonly found. Numerous mature neuron-like tumor cells with a long apical expansion were found throughout the sections. These neuronal cells showed myelin-like configurations

Table 1—Localization and Distribution of Tumors

Case No.	Sex	Days after inoculation	Location of tumors
1	M	37	Th12-L5, dorsal region
2	F	39	L1-L4, dorsal half
3	F	41	L2-S1, dorsal region
4	M	42	Th12-L1, dorsal half
5	F	61	Th12-L4, dorsal half
6	F	55	Small incipient tumor, left rostral corner of lateral ventricle
7	M	57	Small round tumor, right ventral horn
8	F	57	Entire lumen of fourth ventricle, right frontal lobe, small tumors
9	F	60	Right occipital lobe, solid tumors
10	F	60	Right occipital, temporoparietal and spinal cord S-1
11	F	66	Multicentric, right frontal, right occipital, left parietooccipital, fourth ventricle and medulla oblongata
12	F	67	Right parietooccipital
13	M	82	Left olfactory bulb, parietotemporal
14	M	92	Multicentric, left olfactory bulb, left septum pellucidum, left frontoparietal
15	M	92	Left parietooccipital to brachium cerebri
16	F	93	Left olfactory bulb to frontotemporal lobes
17	F	93	Multicentric, large, left intraventricular; small, right anterior horn and right olfactory bulb
18	M	94	Multicentric, both olfactory bulbs, left parietooccipital and fourth ventricle
19	M	99	Dual, right olfactory bulb to frontoparietal and left occipital lobes
20	F	99	Right parietooccipital intraventricular
21	F	129	Dual, right olfactory bulb and bilateral frontoparietal
22	F	151	Fourth ventricle, cerebellar and right cerebellar peduncle
23	M	55	Minute, incipient tumor in right posterior corner of lateral ventricle

Cases with multiple tumors of multicentric origin in both brain and spinal cord are in bold face.

(Figure 9). Intranuclear or intramitochondrial fibrillary rodlets and concentric lamellar bodies were occasionally seen. Intracytoplasmic multivesicular bodies were also common.

Discussion

The uniform phenotype of adenovirus-produced neoplasms in rats is indistinguishable from the phenotype produced by the same viral genome in other animals.[7,9–12] All 23 cases, including 9 rats in which a

multicentric transformation occurred, possessed a remarkably uniform histopathologic picture, apparently triggered simultaneously by a single exposure to the virus. The basic cytology of the tumor has a human counterpart in the medulloepithelioma of children described by Fujita,[13] Willis,[14] Deck [15] and Jellinger.[16] The tendency, observed by Jellinger, of the medulloepithelioma cells to form axon-like argyrophilic processes is also one of the hallmarks of adeno-type neoplasms.

All brain and spinal cord tumors examined contained numerous cells equipped with a solitary cilium which persistently displayed a characteristic 9+0 pattern (Figure 8). This type of cilium is considered typical of sensory neuronal cells. Under normal conditions, cilia with the same morphology are observed in the neural epithelia of the chick embryo,[17] in the differentiating retinal neurons,[18] in fully developed retinae,[19] in hippocampal granular neurons of the dentate fascia of adult rats,[20] in the bipolar neurons of the olfactory bulb of the frog,[21] and in the normal dorsal sensory gray matter of the spinal cord in rats.[22]

The present study includes seven tumors primarily involving the olfactory bulb, twelve hemispherical tumors which almost entirely replaced the right hippocampal convolution, ten tumors which invaded the left hippocampus and twelve tumors affecting the visuosensory cortices. All spinal cord tumors occupied the dorsal sensory column in the lumbosacral segment. This selective propensity of the virus for the dorsal sensory column is more marked in hamsters [9] than in Sprague-Dawley rats. In the fourth ventricle, the alar plate of the medullary velum, which is assumed to supply receptive sensory relay nuclei and peduncles,[23] is definitely contiguous to the tumors which protrude in the ventricle (Figures 3B and 5B). These facts suggest that, in the periventricular zone, developing neuron precursors ordained for the sensory neuronal complex are particularly susceptible to adenovirus oncogenesis.

Zülch [24] emphasized that there is a strong tendency for a large number of chemically induced medulloepitheliomatous tumors to originate in the olfactory nerve of macrosomatic rodents. He suggests that the high population of sensory neuronal epithelia in the rodent olfactory bulb is plausibly related to their susceptibility to chemical carcinogens. Virus fluid introduced in the left frontal lobe has been found to enter the cerebrospinal fluid.[25] Consequently, the proximity of the stratum subependymale ventriculi olfactorii to the rostral horns of the lateral ventricle is an important factor in accounting for the high susceptibility of the olfactory bulb to the virus. Similarly, the definite preference of adeno-type tumors for the hippocampal convolution can be accounted for

by the olfactory function of the rhinencephalon. Although cilia with the same morphology have been observed in human retinoblastoma cells,[18,27,28] astrocytoma cells,[29] and some cells in fibroblastic or endotheliomatous meningiomas,[30] their function in different neoplastic cells remains unexplained.

Intracytoplasmic myelin figures (Figure 9), similar to those described by Tani *et al*[31] in human medulloblastoma, were also prevalent. Such intracytoplasmic myelin figures have rarely been observed in other types of brain tumors fixed with glutaraldehyde and osmium tetroxide. The abundance of phospholipids in adenovirus neoplasms may well support the assumption of Tani *et al*[31] with regard to the morphogenesis of this type of inclusion body. Membranous whorls closely resembling myelin figures have also been observed in cells of the culture explants from spinal ganglion neuroblasts.[32]

The occasional appearance of relatively well-organized neuronal tumor cells may well account for the unusually high cholinesterase activity in adenovirus neoplasms.[33] Although ganglion-cell-like maturation has been recorded in human embryonic brain tumors,[15,16,34] it has never been found associated with a high cholinesterase activity.

The production of adenovirus type 12 T-antigen in medulloepitheliomatous tumors[9] strongly indicates that in adenovirus tumorigenesis, a crucial target-cell determinant may reside in either viral or cellular DNA.[35] Detailed studies of medulloepitheliomatous neoplasms of the rat utilizing immunofluorescein T-antigen detection and experiments involving tumor transplantation into newborn rats will be described in a later paper.

References

1. Kibrick S, Enders JF, Robbins FC: An evaluation of the roller-tube tissue culture for the isolation of poliomyelitis viruses from feces. J Immunol 75: 391–400, 1955
2. Kibrick S, Meléndez L, Enders JF: Clinical association of enteric viruses with particular reference to agents exhibiting properties of the ECHO group. Ann NY Acad Sci 67:311–325, 1957
3. Pereira MS, MacCallum FO: Infection with adenovirus type 12. Lancet 1:198–199, 1964
4. Olson LC, Miller G, Hanshaw JB: Acute infectious lymphocytosis presenting as a pertussis-like illness: its association with adenovirus type 12. Lancet 1:200–201, 1964
5. Yabe Y: Antibody to adenovirus type 12 among infants. Lancet 1:1447–1448, 1964
6. Trentin JJ, Yabe Y, Taylor G: The quest for human cancer viruses. Science 137:835–841, 1962

7. Mukai N, Kobayashi S: Undifferentiated intraperitoneal tumors induced by human adenovirus type 12 in hamsters. Am J Pathol 69:331–348, 1972
8. Karnovsky MJ: A formaldehyde-glutaraldehyde fixative of high osmolarity for use in electron microscopy. J Cell Biol 27:137A, 1965 (Abstr)
9. Mukai N, Kobayashi S: Primary brain and spinal cord tumors induced by human adenovirus type 12 in hamsters. J Neuropathol Exp Neurol (In press) 1973
10. Mukai N, Kobayashi S: Extraocular intraorbital tumors induced by human adenovirus type 12 in hamsters. Invest Ophthalmol 12:185–192, 1973
11. Kobayashi S, Mukai N: Intraocular neurogenic neoplasms induced by human adenovirus type 12 in hamsters. Unpublished data
12. Kobayashi S, Mukai N: Adenovirus-typical tumors produced in C3Hf/Bi and C3H/BifB/ki strains. Unpublished data
13. Fujita S: Medullo-epithelioma: its place in the histogenetic classification of neuro-ectodermal tumors. Acta Pathol Jap 8 (Suppl): 789–794, 1958
14. Willis RA: Pathology of Tumours. The Gliomata, Fourth edition. London, Butterworths, 1967, pp 828–831
15. Deck JHN: Cerebral medulloepithelioma with maturation into ependymal cells and ganglion cells. J Neuropathol Exp Neurol 28:442–454, 1969
16. Jellinger K: Cerebral medulloepithelioma. Acta Neuropathol (Berl) 22: 95–101, 1972
17. Sotelo JR, Trujillo-Cenóz O: Electron microscopic study on the development of ciliary components of the neural epithelium of the chick embryo. Z Zellforsch Mikrosk Anat 49:1–12, 1958
18. Popoff N, Ellsworth RM: The fine structure of nuclear alterations in retinoblastoma and in the developing human retina: *in vivo* and *in vitro* observations. J Ultrastruct Res 29:535–549, 1969
19. Hogan MJ, Alvarado JA, Weddell JE: Histology of the Human Eye: An Atlas and Textbook. Philadelphia, W.B. Saunders Co, 1971, pp 424–444
20. Dahl HA: Fine structure of cilia in rat cerebral cortex. Z Zellforsch Mikrosk Anat 60:369–386, 1963
21. Reese TS: Olfactory cilia in the frog. J Cell Biol 25:209–230, 1965
22. Duncan D, Williams V, Morales R: Centrioles and cilia-like structures in spinal gray matter. Tex Rep Biol Med 21:185–187, 1963
23. Arey LB: Developmental Anatomy: A Textbook and Laboratory Manual of Embryology, Sixth edition. Philadelphia, W.B. Saunders Co., 1959
24. Zülch KJ, Mennel HD: Recent results on chemically induced tumours of the nervous system, Proceedings of the Fourth International Congress of Neuropathology. Paris, Masson et Cie, 1970, pp 60–83
25. Kobayashi S, Mukai N: A sequential study of intracellular T-antigens in newborn Sprague-Dawley rats following single intracerebral inoculation of human adenovirus type 12. Unpublished data
26. Allen RA, Latta H, Straatsma BR: Retinoblastoma: a study of two cases by electron microscopy. Invest Ophthalmol 1:728–744, 1962
27. Ts'O MOM, Fine BS, Zimmerman LE: The nature of retinoblastoma. II. Photoreceptor differentiation: an electron microscopic study. Am J Ophthalmol 69:350–359, 1970
28. Kobayashi S, Mukai N: Human adenovirus induced retinoblastoma-like neoplasms in Sprague-Dawley rats. Invest Ophthalmol, 1973 (In press)

29. Tani E, Higashi N: Ciliated human astrocytoma cells. Acta Neuropathol (Berl) 15:208–219, 1970
30. Cervós-Navarro J, Vázquez J: Electronen-mikroskopische Untersuchungen über das Vorkommen von Cilien in Meningeomen. Virchows Arch [Pathol Anat] 341:280–290, 1966
31. Tani E, Higashi N: Myelin figures associated with the cytoplasmic membranes in human medulloblastoma. Acta Neuropathol (Berl) 21:128–139, 1972
32. Pannese E: Structures possibly related to the formation of new mitochondria in spinal ganglion neuroblasts. J Ultrastruct Res 15:57–65, 1966
33. Schachner M, Chaffee J, Kobayashi S, Mukai N: A quantitative assessment of cholinesterase activity in the tissue culture explant from adenovirus typical neoplasms. Unpublished data
34. Mukai N: An evaluation of gliomas derived from the ependymal anlage. J Neuropathol Exp Neurol 15:33–60, 1956
35. Green M, Fujinaga K, Piña M, Thomas DC: Molecular basis of viral oncogenesis, Exploitable Molecular Mechanisms and Neoplasia. Baltimore, Williams and Wilkins, Co, 1969, pp 479–506

Acknowledgments

This work is dedicated to our great teacher, the late Professor Emeritus Tomizo Yoshida, MD, whose dedication and leadership in cancer research will not be forgotten.

We are indebted to Dr. Charles Schepens, Head of the Department of Retina Research at the Retina Foundation, and Professor H. M. Zimmerman, Chief of Pathology at the Montefiore Hospital, New York, for invaluable criticism and advice. Dr. Masami Oguri, Mrs. Elizabeth Newcomb and Miss Ruiko Kato provided excellent technical assistance; Mr. David F. Dobies provided editorial assistance.

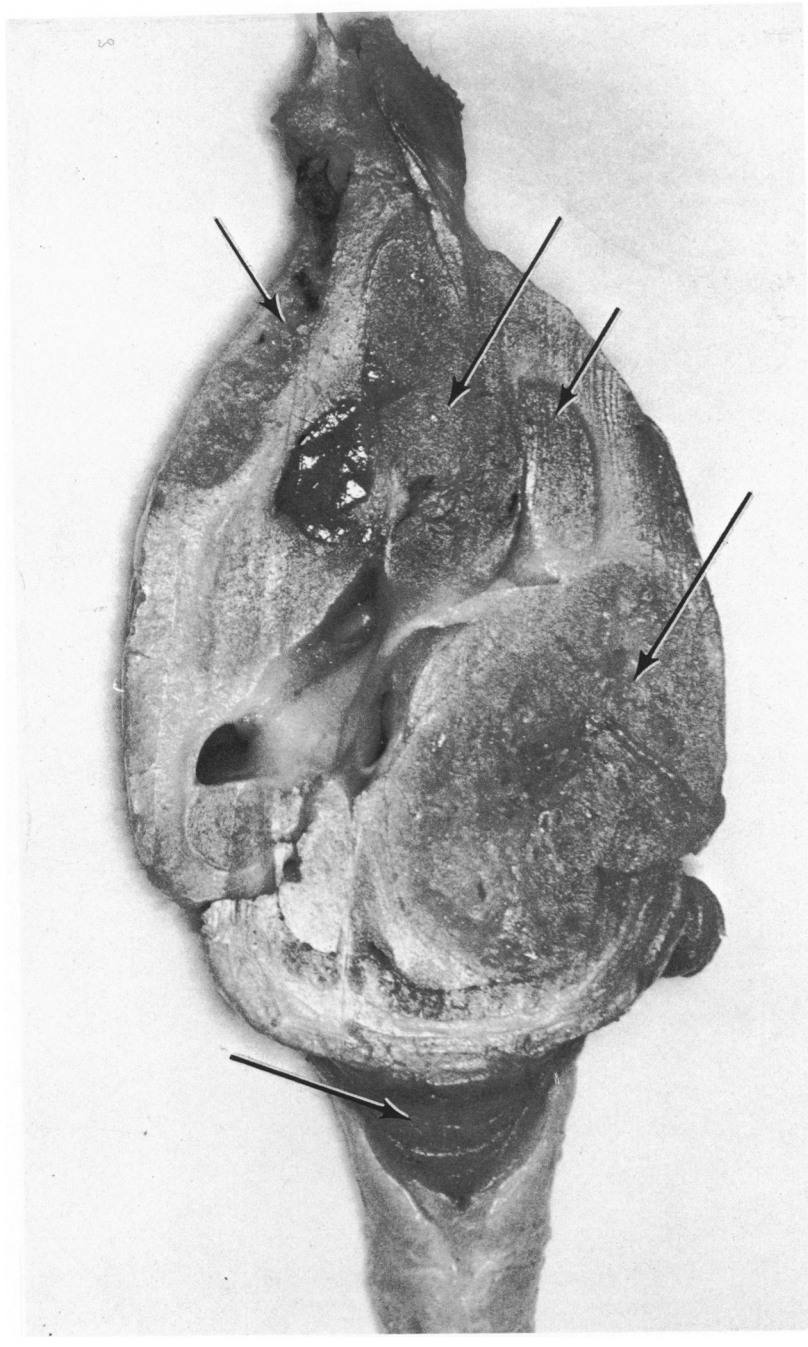

Fig 1—Multiple tumors arising simultaneously from the olfactory bulb to the floor of the fourth ventricle. *Arrows* point out five entirely independent tumors.

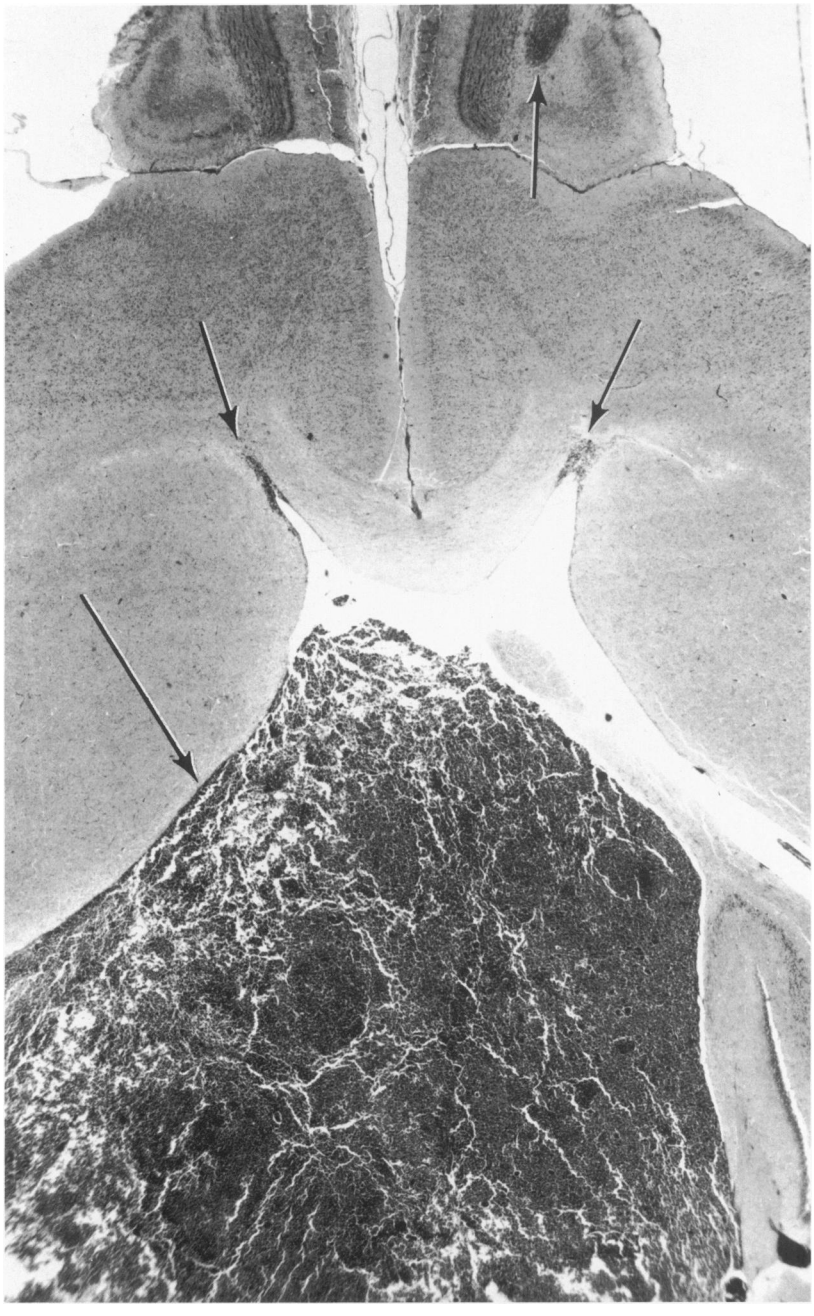

Fig 2—A large intraventricular tumor partly attached to a rudimentary cell cluster in the periventricular zone (*long arrow*). Note minute incipient foci of transformed cells (*short arrows*) in both the ventral horns and right olfactory bulb (PTAH, × 10).

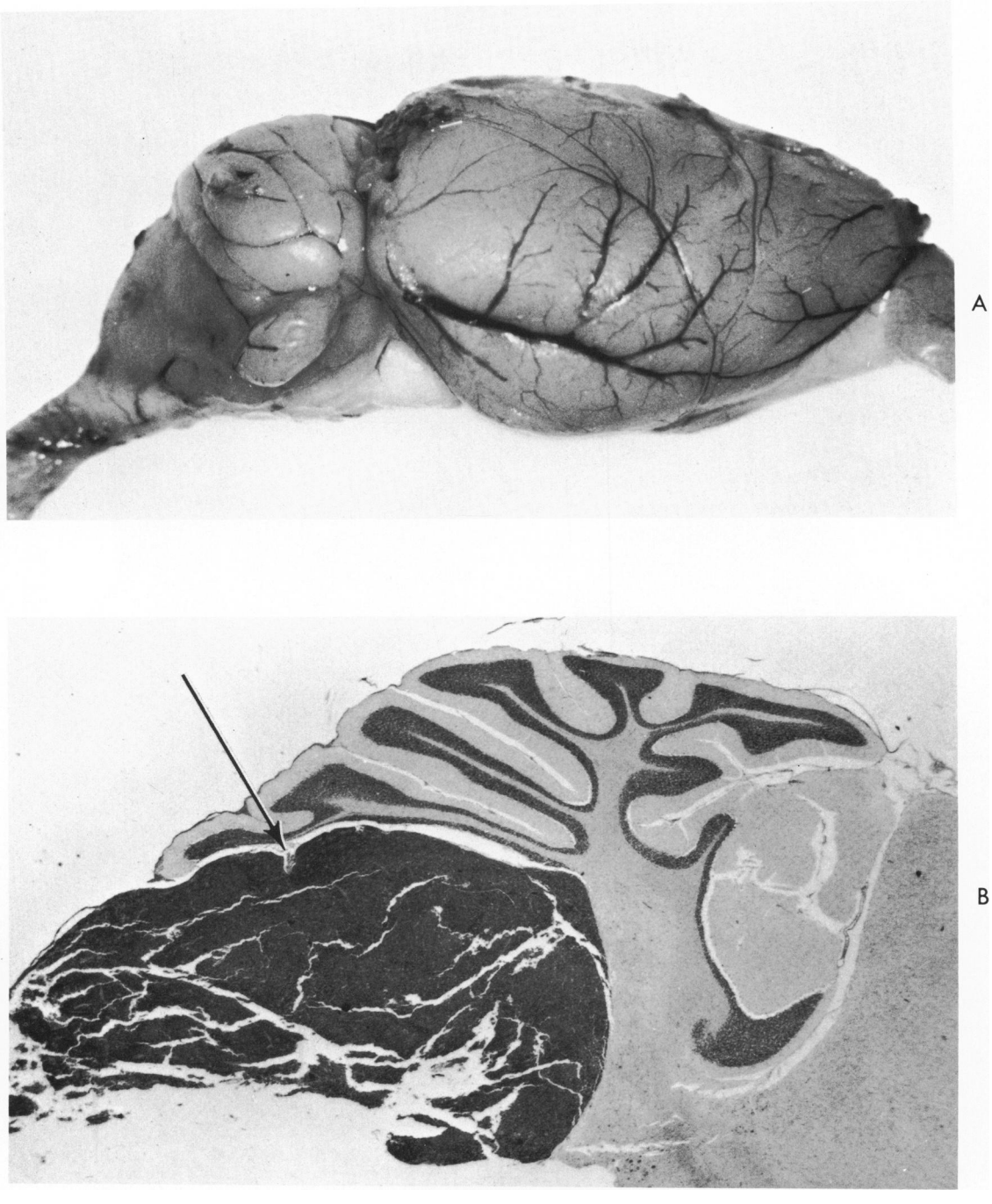

Fig 3A—Tumor mass which replaced a part of the cerebellar folia. **B**—Sagittal section of the tumor showing a partial neoplastic encroachment of the uvula vermis and nodulus. Note the apparent contiguity of the tumor and the tela choroidea (*arrow*) (H&E, × 7).

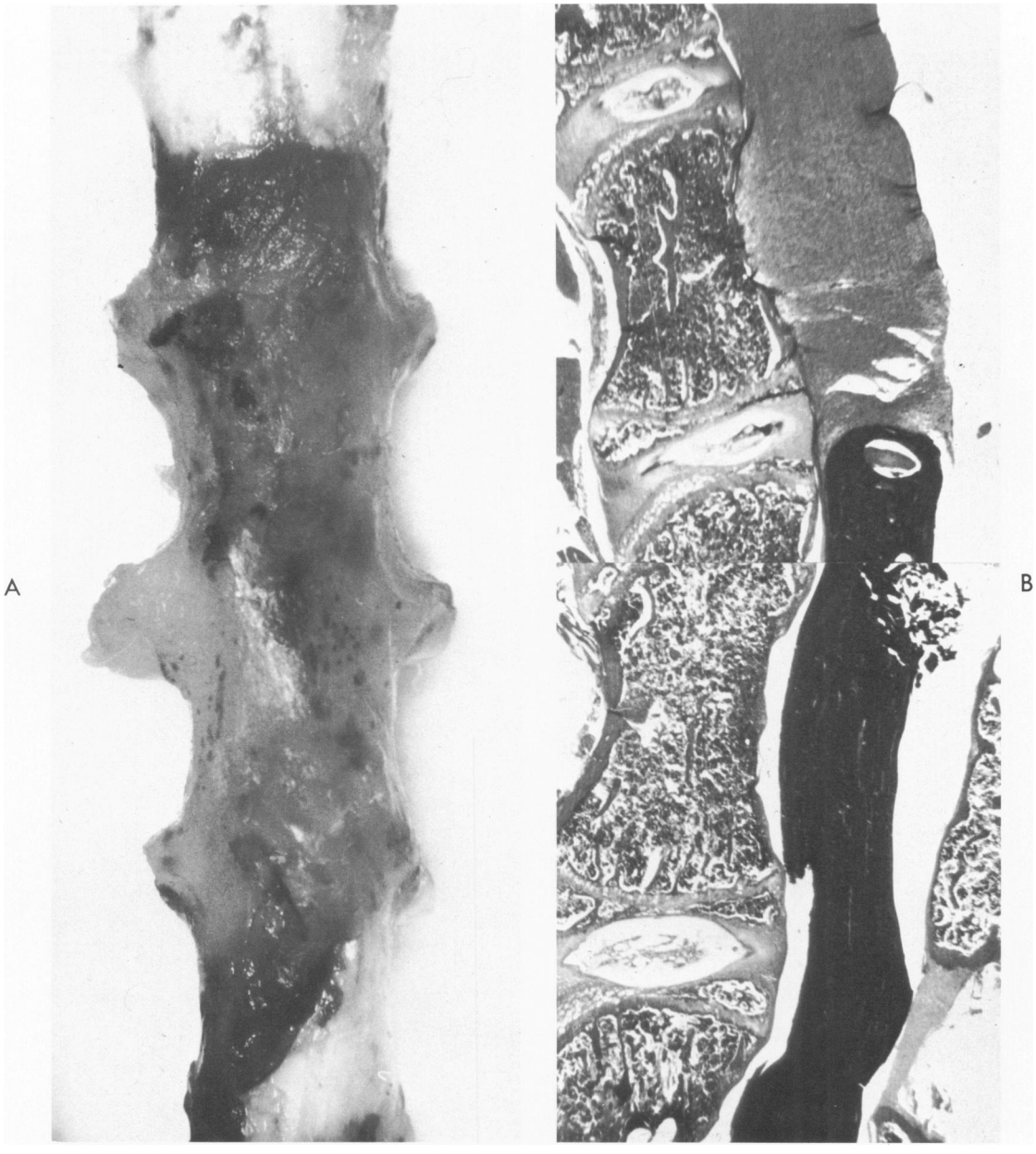

Fig 4A—*In situ* replacement of a lumbosacral segment of the spinal cord with neoplastic tissue. Note the autochthonous neoplastic transformation of otherwise well-preserved dorsal spinal nerve roots. **B**—Sagittal section of the tumor showing the entire replacement of the lumbosacral segment with neoplastic cells (H&E, × 40).

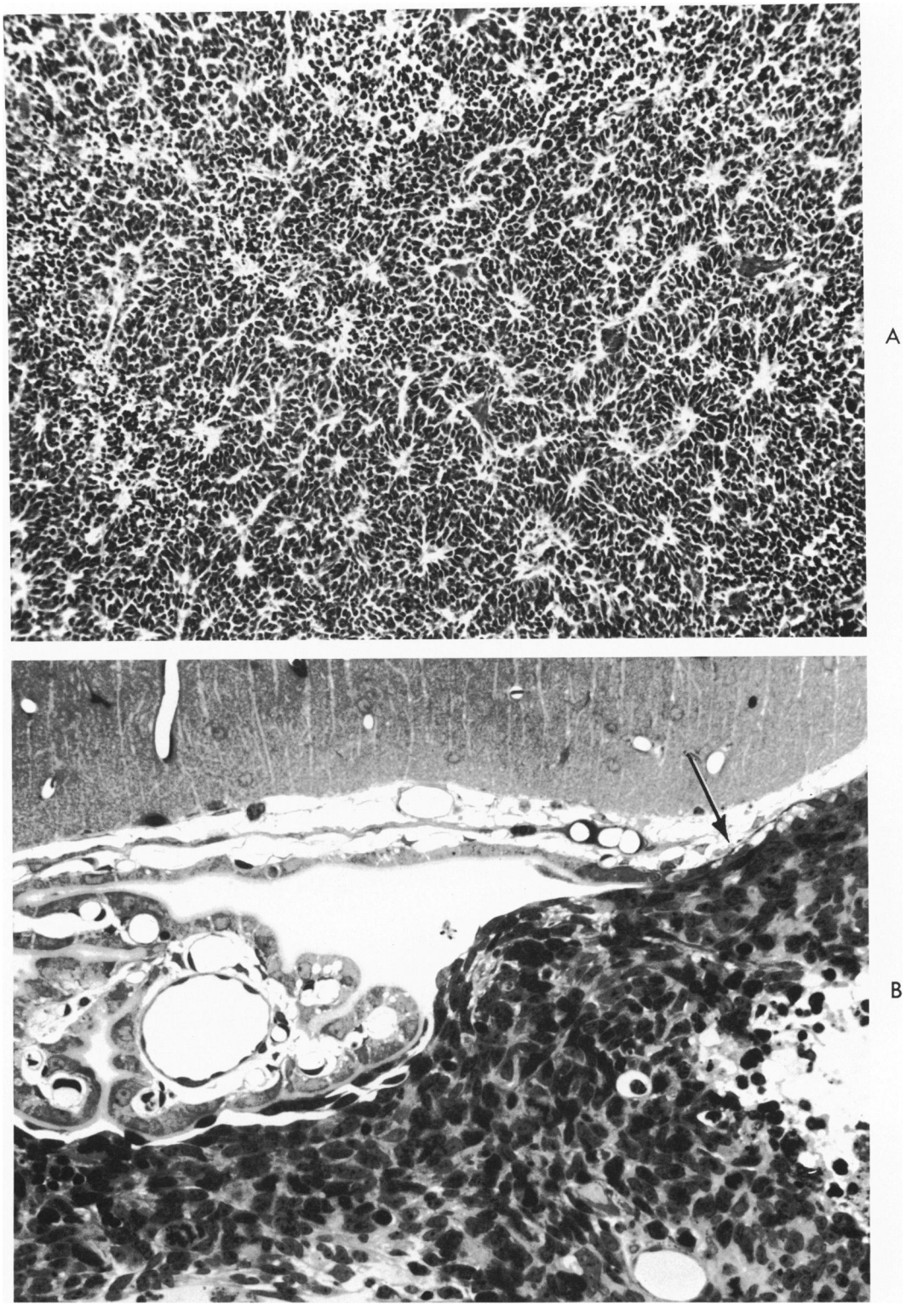

Fig 5A—Low-power view of an adenovirus typical neoplasm depicting the remarkably uniform histopathology with numerous rosettes, pararosettes and a solid mosaic cell pattern (H&E, × 100). **B**—Typical tumor cells merging with a cluster of transitional atypical cells of the tela choroidea and a part of the velum medullare (*arrow*, compare with Figure 3B) (Toluidine blue, × 300).

Fig 6A—Uniform argentaffinity of tumor cells revealing an apparent lack of connective tissue stroma throughout the tissue (Foot's reticulin silver stain, × 120).

Fig 6B—Argyrophile fibrils, with or without a fine spine-like protuberance, arising from many neuronal tumor cells. Intracytoplasmic neurofibril-like particles were also common (Holmes' silver impregnation, × 1000).

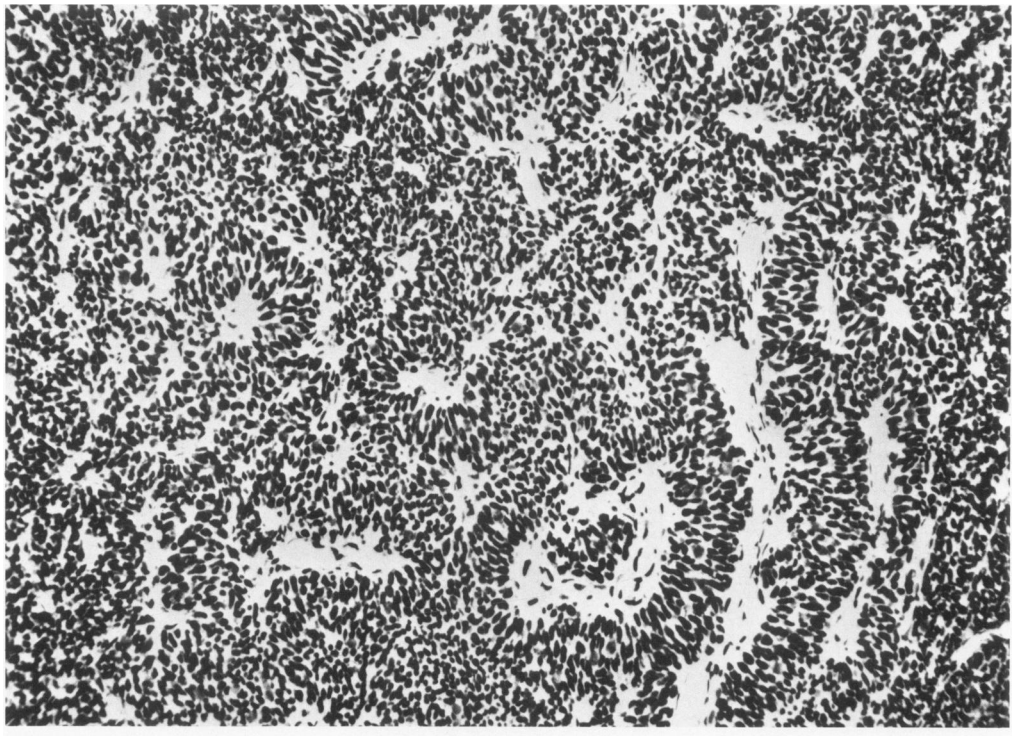

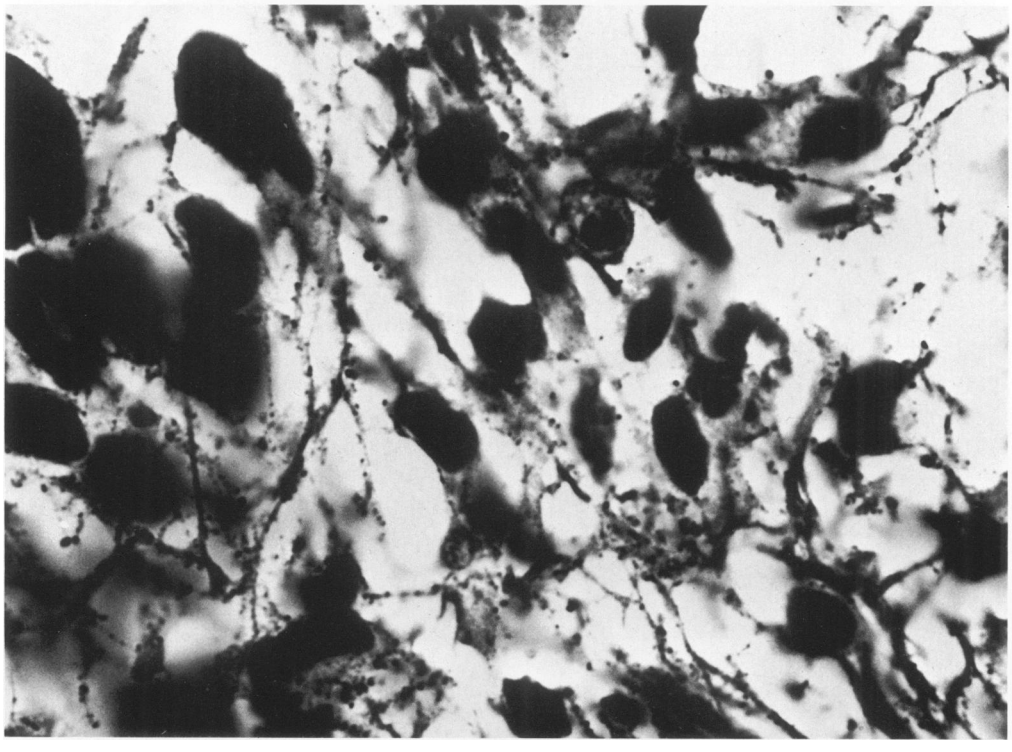

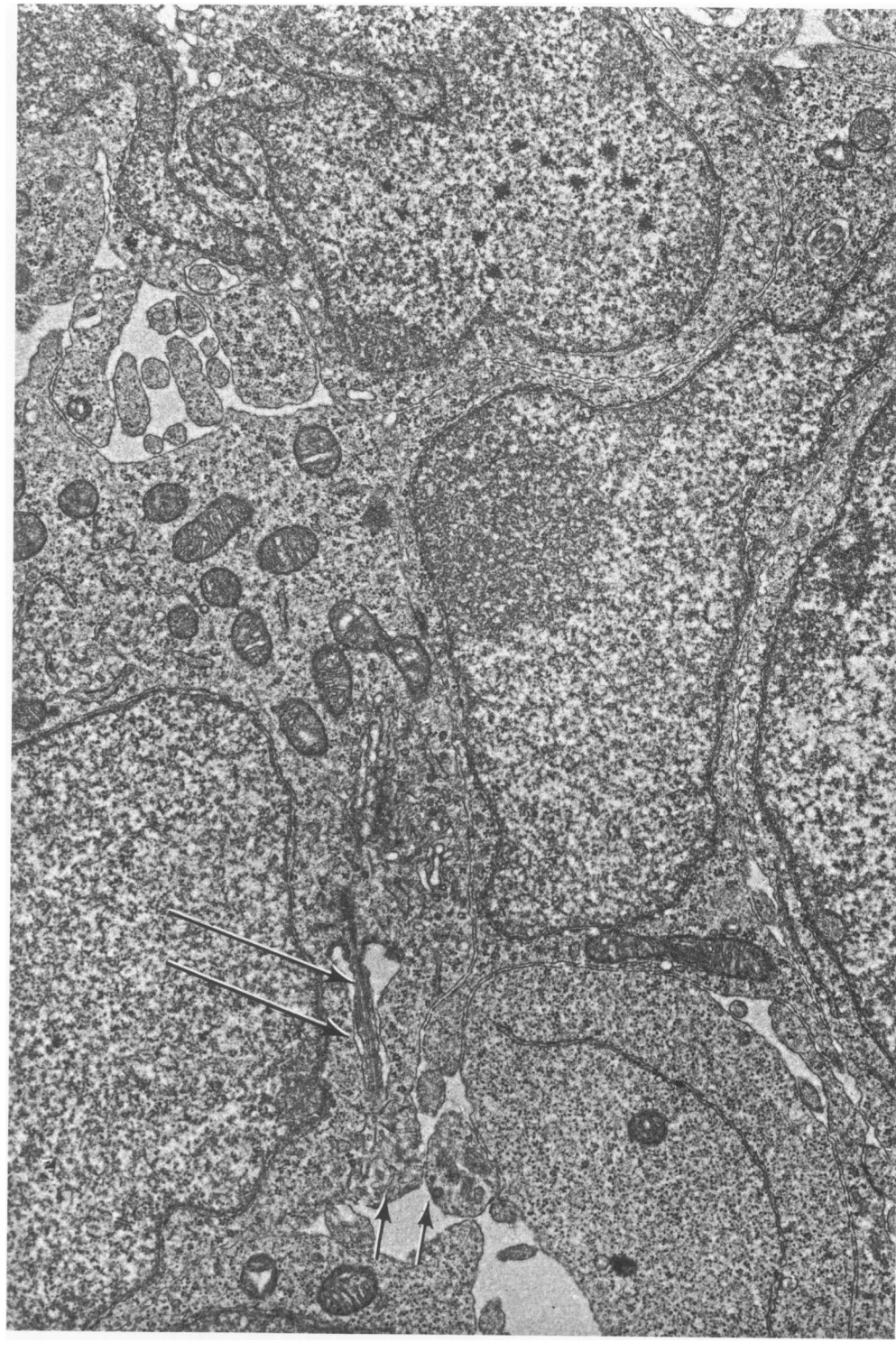

Fig 7—Electron microscopy of tumor cells showing moderately indented nuclei with poorly differentiated cytoplasmic organelles. Polarization of mitochondria in the apical processes, numerous microtubules in the villose cell expansions (*short arrows*) and solitary cilium (*long arrows*) are common features (× 12,500).

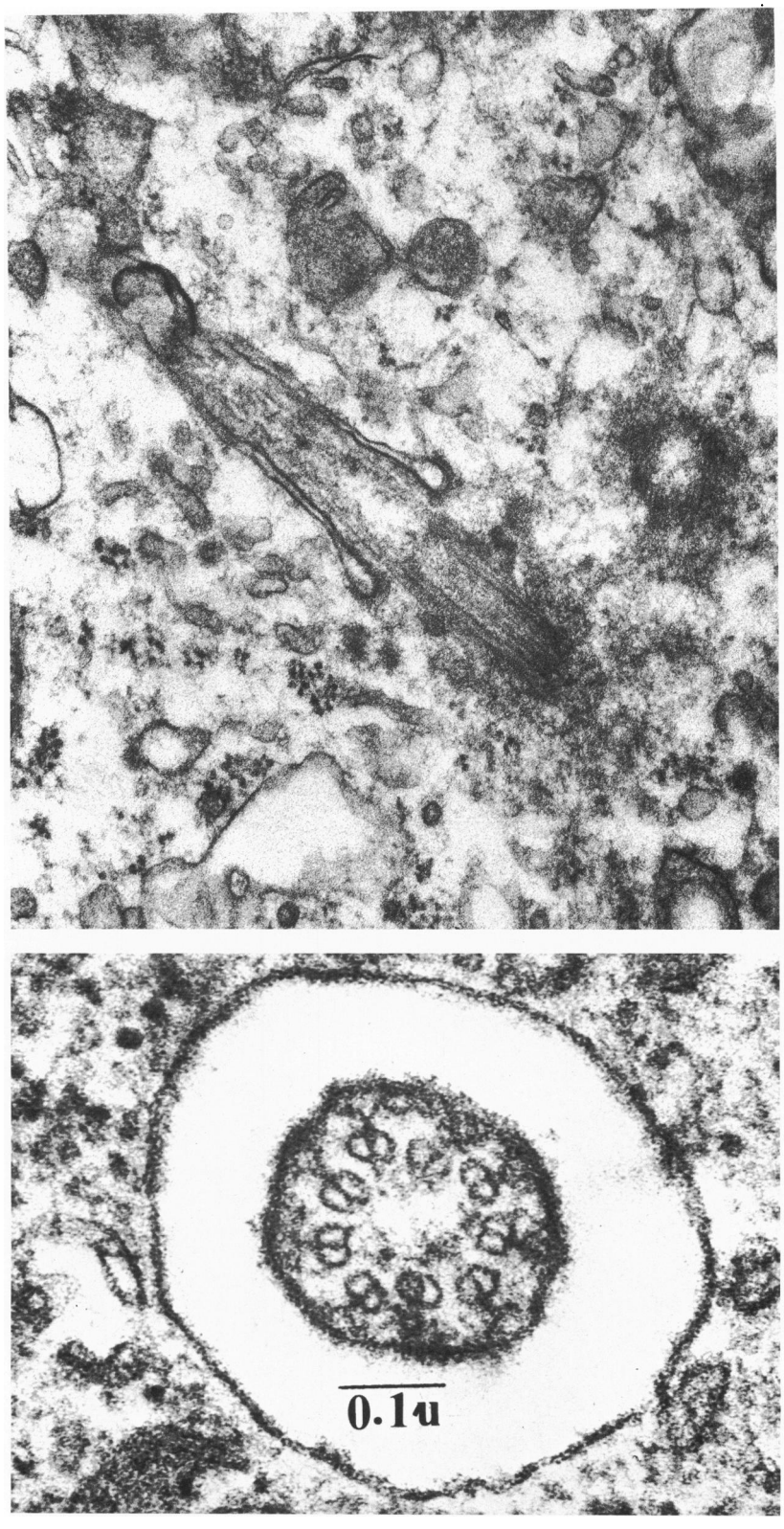

Fig 8A—Longitudinal section of typical solitary cilium and its associated centriole. Note spoke-like prolongations at the intracytoplasmic projection (× 23,000). **B**—Cross section of the cilia persistently reveals a 9 + 0 pattern, the structural analog of cilia performing a sensory function (× 71,000).

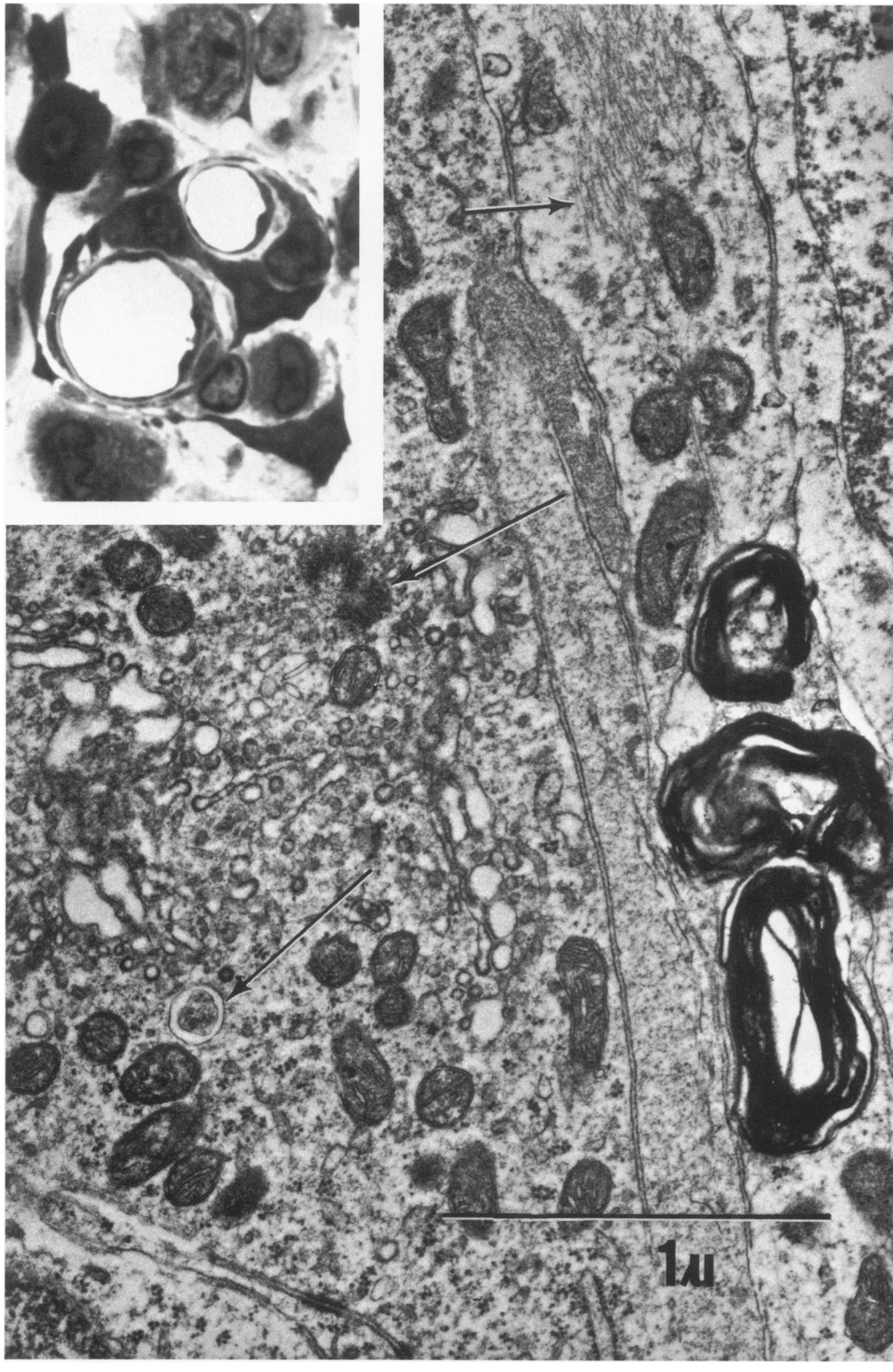

Fig 9—Characteristic myelin figures prevailed in the ganglionic tumor cell cytoplasm. Note the anomalous cilium and centrioles (*long arrows*). Neurofilamentous profiles (*short arrow*) are common in these ganglionic tumor cells (× 23,000). **Inset**—Ganglionic tumor cells (Toluidine blue, × 1000).